RAA 2016 Vol. **16** No. **5**, 79 (6pp) doi: 10.1088/1674–4527/16/5/079
http://www.raa-journal.org *http://iopscience.iop.org/raa*

***R**esearch in*
***A**stronomy and*
***A**strophysics*

On the variable timing behavior of PSR B0540−69: an almost excellent example to study the pulsar braking mechanism

Fei-Fei Kou[1,2], Zi-Wei Ou[1,2] and Hao Tong[1]

[1] Xinjiang Astronomical Observatory, Chinese Academy of Sciences, Urumqi 830011, China; *tonghao@xao.ac.cn*
[2] University of Chinese Academy of Sciences, Beijing 100049, China

Received 2015 September 10; accepted 2015 December 4

Abstract PSR B0540−69 has a braking index measurement in its persistent state: $n = 2.129 \pm 0.012$. Recently, it has been reported to have changes in its spin-down state: a sudden 36% increase in the spin-down rate. Combining the persistent state braking index measurement with different spin-down states, PSR B0540−69 is more powerful than intermittent pulsars in constraining pulsar spin-down models. The pulsar wind model is applied to explain the variable timing behavior of PSR B0540−69. The braking index of PSR B0540−69 in its persistent state results from the combined effect of magnetic dipole radiation and particle wind. The particle density reflects the magnetospheric activity in real-time and may be responsible for the changing spin-down behavior. Corresponding to the 36% increase in the spin-down rate of PSR B0540−69, the relative increase in the particle density is 88% in the vacuum gap model. The braking index calculated with the model in the new state is $n = 1.79$. Future observations that measure the braking index of PSR B0540−69 in the new spin-down state will be very powerful in distinguishing between different pulsar spin-down models and different particle acceleration models in the wind braking scenario. The variable timing behavior of PSR J1846−0258 is also understandable in the pulsar wind model.

Key words: pulsars: general — pulsars: individual (PSR B0540−69; PSR J1846−0258) — stars: neutron — wind

1 INTRODUCTION

PSR B0540−69, known as the "Crab Twin," is a young radio pulsar with spin-down parameters $\nu \approx 19.727\,\mathrm{Hz}$, $\dot{\nu} \approx -1.86 \times 10^{-10}\,\mathrm{Hz\,s^{-1}}$ (Marshall et al. 2015) and braking index $n = 2.129 \pm 0.012$ (Ferdman et al. 2015). Its characteristic magnetic field is about $10^{13}\,\mathrm{G}$ at the magnetic poles[1]. Only two glitches with relatively small changes in spin-down rate have been reported (Zhang et al. 2001; Cusumano et al. 2003; Livingstone et al. 2005; Ferdman et al. 2015). Recently, a persistent and unprecedented increase in the spin-down rate of PSR B0540−69 was observed: the relative increase in the spin-down rate was 36% which is orders magnitude larger than the changes induced by glitches (Marshall et al. 2015). Another pulsar, PSR J1846−0258, was also reported to have variable timing behaviors with a net decrease in the spin frequency ($\Delta\nu \approx -10^4\,\mathrm{Hz}$) after the large glitch (Livingstone et al. 2010) and a lower braking index of $n = 2.19 \pm 0.03$ (Livingstone et al. 2011; Archibald et al. 2015a) than its persistent state value of $n = 2.65 \pm 0.01$ (Livingstone et al. 2006).

[1] This assumes all of the rotational energy is consumed by magneto-dipole radiation in a vacuum such that $B(\mathrm{pole}) = 6.4 \times 10^{19}\sqrt{P\dot{P}}\,\mathrm{G}$.

The spin-down behavior of pulsars can be described by the power law

$$\dot{\nu} = -C\nu^n, \tag{1}$$

where ν and $\dot{\nu}$ are respectively the spin frequency and frequency derivative; C is usually taken as a constant and n is the braking index. The braking index is defined accordingly

$$n = \frac{\nu\ddot{\nu}}{\dot{\nu}^2}, \tag{2}$$

where $\ddot{\nu}$ is the second derivative of spin frequency. The braking index reflects the pulsar braking mechanism (Tong 2015). In the magneto-dipole braking model, a pulsar rotates uniformly in a vacuum such that $\dot{\nu} \propto \nu^3$. The expected braking index is three which is not consistent with observations (Lyne et al. 2015). Like in the case of intermittent pulsars (Kramer et al. 2006), PSR B0540−69 also has two different spin-down states. For the intermittent pulsar PSR B1931+24, researchers have tried to measure its braking index during the on and off states (Young et al. 2013). Now this aim has been partially fulfilled by PSR B0540−69 which not only has different spin down states but also a measurement of the braking index for the persistent state ("low" spin-down rate state), see Table 1.

Therefore, it can be used to put more constraints on pulsar spin-down models. Any candidate model should explain both the braking index during the persistent state and the variable spin-down rate.

Previously, the pulsar wind model (Xu & Qiao 2001) was employed to explain the spin-down behavior of intermittent pulsars (Li et al. 2014) and the braking index of the Crab pulsar (Kou & Tong 2015). In the following, it is shown that both the braking index in the persistent state and varying spin-down rate of PSR B0540−69 are also understandable in the wind braking model. The varying spin-down rate is due to a variable particle wind. The varying braking index of PSR J1846−0258 is caused by a changing particle density. The pulsar wind model and related calculations are listed in Section 2. Discussions and conclusions are presented in Section 3 and Section 4, respectively.

2 VARIABLE TIMING BEHAVIOR OF PULSARS CAUSED BY A VARYING PARTICLE WIND

2.1 Description of the Pulsar Wind Model

In general, pulsars are oblique rotators. The perpendicular and parallel magnetic dipole moments may, respectively, be related to the magnetic dipole radiation and acceleration of particles (Xu & Qiao 2001; Kou & Tong 2015)

$$\dot{E}_{\rm d} = \frac{2\mu^2\Omega^4}{3c^3}\sin^2\alpha\,, \tag{3}$$

$$\dot{E}_{\rm p} = 2\pi r_{\rm p}^2 c\rho_{\rm e}\Delta\phi = \frac{2\mu^2\Omega^4}{3c^3}3\kappa\frac{\Delta\phi}{\Delta\Phi}\cos^2\alpha\,, \tag{4}$$

where $\mu = 1/2BR^3$ is the magnetic dipole moment (B is the polar magnetic field and R is the neutron star radius), c is the speed of light, and α is the angle between the rotational axis and the magnetic axis (i.e. inclination angle), $\Omega = 2\pi\nu$ is the angular velocity of the pulsar, $r_{\rm p} = R(R\Omega/c)^{1/2}$ is the polar cap radius, $\rho_{\rm e} = \kappa\rho_{\rm GJ}$ is the primary particle density where $\rho_{\rm GJ} = \Omega B/(2\pi c)$ is the Goldreich-Julian charge density (Goldreich & Julian 1969) and κ is the dimensionless particle density, $\Delta\phi$ is the corresponding acceleration potential of the acceleration region, and $\Delta\Phi = \mu\Omega^2/c^2$ is the maximum acceleration potential for a rotating dipole (Ruderman & Sutherland 1975). The rotational energy of the pulsar is consumed by the combined effect of magnetic dipole radiation and particle acceleration (Xu & Qiao 2001)

$$-I\Omega\dot{\Omega} = \frac{2\mu^2\Omega^4}{3c^3}\eta\,, \tag{5}$$

where $I = 10^{45}\,{\rm g\,cm^2}$ is the moment of inertia and

$$\eta = \sin^2\alpha + 3\kappa\Delta\phi/\Delta\Phi\cos^2\alpha\,. \tag{6}$$

The spin-down behavior can be expressed as

$$\dot{\Omega} = -\frac{2\mu^2\Omega^3}{3Ic^3}\eta\,. \tag{7}$$

According to Equation (2), the braking index in the pulsar wind model can be written as (Xu & Qiao 2001)

$$n = 3 + \frac{\Omega}{\eta}\frac{d\eta}{d\Omega}\,. \tag{8}$$

The exact expression of η (Eq. (6)) depends on the potential of the acceleration gap. The vacuum gap model (Ruderman & Sutherland 1975) is taken as an example to show the calculation process and

$$\eta = \sin^2\alpha + 4.96\times10^2\kappa B_{12}^{-8/7}\Omega^{-15/7}\cos^2\alpha\,, \tag{9}$$

where B_{12} is the magnetic field in units of $10^{12}\,{\rm G}$ (Kou & Tong 2015). For other acceleration models, the corresponding expressions of η are listed in table 2 of Kou & Tong (2015).

2.2 On the Variable Timing Behavior of PSR B0540−69

A generic picture for the variable timing behavior of PSR B0540−69 and PSR J1846−0258 is: a glitch may have occurred during the observations, like what happened in PSR J1846−0258 (Livingstone et al. 2010). This small glitch could have been missed in the case of PSR B0540−69. This glitch might have induced some magnetospheric activities, e.g. outburst (Gavriil et al. 2008). The particle outflow would be stronger during this process. This will cause the pulsar to have a larger spin-down rate (Marshall et al. 2015). After some time, a larger spin-down state will result in a net spin-down of the pulsar compared with previous timing solutions (Livingstone et al. 2010). The braking index will be smaller since the particle wind is stronger (Wang et al. 2012a). When the pulsar magnetosphere relaxes to its persistent state, if the particle density is still varying with time $\kappa = \kappa(t)$, the braking index will be different from the persistent state. However, the spin-down rate may not change obviously in this case because the change of the total particle density is small (Livingstone et al. 2011; Archibald et al. 2015a; Kou & Tong 2015). From previous observations of PSR J1846−0258, its pulse profile had no significant variations before, during or after the outburst (Livingstone et al. 2010, 2011; Archibald et al. 2015a). The observations of magnetar 1E 1048.1−5937 have shown that the pulsed flux may not be a good indicator of magnetospheric activities (Archibald et al. 2015b). The variation of total X-ray flux is needed. Therefore, the enhanced spin-down rate in PSR B0540−69 without changes in pulse profile or pulsed flux is not unusual (Marshall et al. 2015). The reason may be that the geometry of the pulsar is unchanged during magnetospheric activities. This may result in a constant pulse profile and pulsed flux.

For the persistent state of PSR B0540−69, we adopt the state spin-down parameters $\nu = 19.727\,{\rm Hz}$, $\dot{\nu} = -1.86\times10^{-10}\,{\rm Hz\,s^{-1}}$ (Marshall et al. 2015) and inclination angle $\alpha = 50^\circ$ (the best fitting value given by Zhang & Cheng 2000). Parameters of magnetic field $B = 10^{13}\,{\rm G}$

Table 1 Comparison of spin-down parameters of PSR B1931+24, PSR B0540−69 and PSR J1846−0258. The intermittent pulsar PSR B1931+24 has different spin-down states but no information about the braking index is known at present. PSR B0540−69 has both different spin-down states and measurements of the braking index in the persistent state. PSR J1846−0258 is reported to have a variation in its braking index.

Pulsar name	ν(Hz)	$\dot{\nu}$(Hz s^{-1})	Braking index
B1931+24 (off)[a]	1.229	-10.8×10^{-15}	?
B1931+24 (on)[a]	1.229	-16.3×10^{-15}	?
B0540−69 (low)[b]	19.727	-1.86×10^{-10}	2.129[c]
B0540−69 (high)[b]	19.701	-2.53×10^{-10}	?
J1846−0258 (persistent state)[d]	3.08	-6.72×10^{-11}	2.65
J1846−0258 (after glitch)[e]	3.06	-6.65×10^{-11}	2.19

Notes: (a) From Kramer et al. (2006). The on state has a larger spin-down rate than the off state. (b) From Marshall et al. (2015). "Low" means the previous spin-down state and "high" means the new spin-down state with a higher spin-down rate. (c) Mean value of braking index (Ferdman et al. 2015). (d) From Livingstone et al. (2006). (e) From Archibald et al. (2015a).

and $\kappa = 834$ can be calculated (by solving Eqs. (5) and (8)) corresponding to the observed braking index $n = 2.129 \pm 0.012$ (Ferdman et al. 2015). The calculated $\kappa = 834$ means that the particle density is 834 times the Goldreich-Julian charge density, which is consistent with previous conclusions (Kou & Tong 2015 and references therein).

The spin-down rate of PSR B0540−69 has increased by 36% in the new spin-down state (Marshall et al. 2015). In the pulsar wind model, the variation of the spin-down rate is caused by a different particle density

$$\frac{\dot{\Omega}'}{\dot{\Omega}} = \frac{\eta(\kappa')}{\eta(\kappa)}\,, \tag{10}$$

where $\dot{\Omega}'$ and $\eta(\kappa')$ correspond to the new spin-down state. A larger particle density will result in a higher spin-down rate (Eqs. (7) and (9)). Figures 1 and 2 show respectively the normalized spin-down rate $\dot{\nu}'/\dot{\nu}$ and braking index as a function of normalized particle density κ'/κ for PSR B0540−69 in the vacuum gap model. As shown in Figure 1, the spin-down rate increases as the particle density increases. An increase in the particle density of 88% will result in an increase of 36% in the spin-down rate. As particle density increases, the braking index will decrease because the effect of the particle wind component is increasing (Fig. 2). When the particle density increases to 1.88 times the previous value, the braking index decreases to 1.79, so the relative change is 15.7%. Also, the corresponding frequency second derivative will be $\ddot{\nu} = 5.83\times10^{-21}\,\mathrm{Hz\,s^{-2}}$ (Eq. (2)).

Calculations are also made in all of the acceleration models. The same conclusion is obtained from these models: an increase in particle density results in an increase in spin-down rate. For PSR B0540−69, corresponding to the observed 36% relative increase in spin-down rate, the relative increase in the particle density in all these models ranges from 72% to 154%. The second frequency derivative ranges from $4.5\times10^{-21}\,\mathrm{Hz\,s^{-2}}$ to $6.15\times10^{-21}\,\mathrm{Hz\,s^{-2}}$. Braking indices in the new state in all these acceleration models are listed in Table 2. If the conversion efficiency of particle energy to X-ray luminosity is unchanged (Becker 2009), the total X-ray luminosity may also have increased by the same factor.

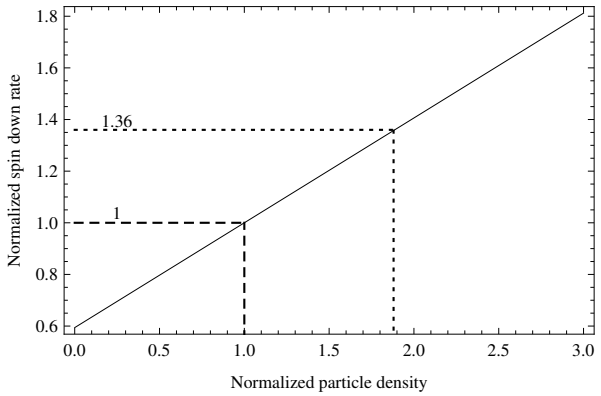

Fig. 1 The normalized spin-down rate as a function of normalized particle density for PSR B0540−69 in the vacuum gap model. The dashed line is the spin-down rate in the persistent state. The dotted line is the new spin-down rate which is 1.36 times the spin-down rate in the persistent state (Marshall et al. 2015).

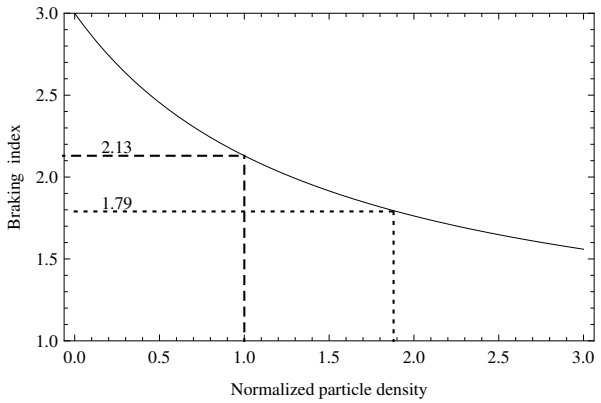

Fig. 2 Braking index as a function of the normalized particle density for PSR B0540−69 in the vacuum gap model. The dashed line is the braking index 2.13 in the persistent state (Ferdman et al. 2015). The dotted line is the braking index 1.79 which is predicted by the increased particle density.

2.3 On the Variable Timing Behaviors of PSR J1846−0258

Spin-down parameters and the persistent state braking index of PSR J1846−0258 are respectively: $\nu = 3.08$ Hz and $\dot{\nu} = -6.72\times10^{-11}\,\mathrm{Hz\,s^{-1}}$, and $n = 2.65\pm0.01$ (Table 1)

Table 2 Braking Indices of PSR B0540−69 in the New State in all the Acceleration Models

Acceleration models	VG(CR)	VG(ICS)	SCLF(II,CR)	SCLF(I)	OG	CAP	NTVG(CR)	NTVG(ICS)
Braking index	1.79	1.87	1.90	1.79	1.38	1.83	1.90	1.86

Notes: See table 2 of Kou & Tong (2015) for the meanings of the abbreviations associated with the acceleration models. The minimum braking index of SCLF (II ICS) is 2.4 (Li et al. 2014) which is larger than the persistent braking index of PSR B0540−69: $n = 2.129$. It means that the SCLF (II, ICS) model can be ruled out or cannot exist alone to accelerate particles in the magnetosphere of PSR B0540−69 (Wu et al. 2003; Li et al. 2014).

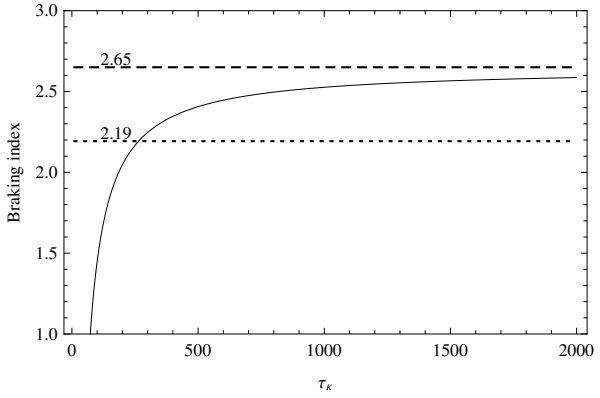

Fig. 3 The braking index of PSR J1846−0258 as a function of τ_κ in the vacuum gap model. The dashed line is the persistent state braking index of 2.65 (Livingstone et al. 2006). The dotted line is the smaller braking index of 2.19 measured after the glitch (Archibald et al. 2015a).

(Livingstone et al. 2006). In the pulsar wind model, corresponding to the observational braking index, the magnetic field $B = 1.25 \times 10^{14}$ G and particle density $\kappa = 28$ are calculated in the vacuum gap model with an inclination angle of 45° (an inclination angle of 45° is chosen in the following calculations[2]). Such a magnetic field is comparable with a characteristic magnetic field of 9.7×10^{13} G at the poles and is much larger than magnetic fields of normal pulsars. Then it is not surprising that magnetar activities can be observed in this source (Gavriil et al. 2008).

Variable timing behavior that shows a net decrease in the spin-down frequency ($\Delta\nu \approx -10^{-4}$ Hz) was detected for PSR J1846−0258 after a larger glitch (Livingstone et al. 2010). The correspondingly relative increase in the spin-down rate is about 7% ($\Delta\dot{\nu} = -4.82 \times 10^{-12}\,\mathrm{Hz\,s^{-1}}$ during an epoch of 240 days when phase coherency was lost). Such an increase in spin down rate may also be caused by a larger particle density. Just like the calculation for PSR B0540−69, in the vacuum gap model of the pulsar wind model, a 44% increase in the particle density results in the 7% increase in the spin-down rate. The braking index will also be smaller during this enhanced spin-down epoch. However, measurement of the braking index can only be made long after the glitch when the timing noise is greatly reduced.

A lower braking index of 2.19 ± 0.03 is detected after the glitch (Livingstone et al. 2011; Archibald et al. 2015a) which is significantly smaller than its persistent state value of $n = 2.65 \pm 0.01$ (Livingstone et al. 2006). In the pulsar wind model, it can be understood by a time varying particle density $\kappa = \kappa(t)$ (similar to the Crab pulsar, Kou & Tong 2015)

$$n = 3 + \frac{\Omega}{\eta}\frac{d\eta}{d\Omega} - \frac{\kappa}{\eta}\frac{d\eta}{d\kappa}\frac{\tau_{\rm c}}{\tau_\kappa}, \qquad (11)$$

where $\tau_{\rm c} = -\frac{\Omega}{2\dot{\Omega}}$ is the characteristic age and $\tau_\kappa = \frac{\kappa}{2\dot{\kappa}}$ is the typical variation timescale of the particle density. An increasing particle density ($\tau_\kappa > 0$ or $\dot{\kappa} > 0$) leads to a smaller braking index. From Figure 3, the braking index is insensitive to τ_κ when it is much larger than 1000 yr, but decreases sharply when τ_κ is comparable to the characteristic age (about 700 yr). The rate of change of the particle density $\dot{\kappa} = 1.68 \times 10^{-9}\,\mathrm{s^{-1}}$ will result in a braking index of 2.19. During the epoch from MJD 55369 to MJD 56651, the particle density has increased 0.66%. The relative increase in spin-down rate is 0.1% which is very small. Therefore, the changing particle density will mainly result in a different braking index but not affect the spin-down rate. This is the difference between the variable timing behavior of PSR 0540−69 and PSR J1846−0258.

3 DISCUSSION

Observations of intermittent pulsars (Kramer et al. 2006) and measurement of braking indices (Lyne et al. 2015) help to distinguish between different pulsar spin-down mechanisms. The variable spin-down rate of PSR B0540−69 combined with a measurement of its braking index in the persistent state is more powerful than intermittent pulsars in constraining different models. In the magneto-dipole radiation model where $\dot{\nu} \propto \mu^2 \sin^2\alpha / I \times \nu^3$, in order to explain the braking indices ($n < 3$) of eight young pulsars, an increasing inclination angle (Lyne et al. 2013), increasing magnetic field (Espinoza et al. 2011) or decreasing moment of inertia (Yue et al. 2007) is expected. The variable spin-down rate may be induced by the change in inclination angle, magnetic field or moment of inertia. Corresponding to the 36% relative increase in the spin-down rate, the relative change should be: a 26% increase in inclination angle, 17% increase in magnetic field, or 26% decrease in moment of inertia. It seems impossible to achieve such huge changes during a short timescale (about 14 days, Marshall et al. 2015). A change in inclination angle is unlikely since the pulse profile did not change significantly (Marshall et al. 2015). An increase in magnetic field would require an increase of magnetic energy by 36%, about 10^{42} erg. It is unlikely that there is such a huge amount of energy injection. A decrease in moment of inertia would require a decrease in neutron star radius. During

[2] There is no observational or best fitting inclination angle given.

this process, a huge amount of gravitational energy would be released (Zhou et al. 2014), about $10^{52}\,\mathrm{erg}$, which is again unlikely.

Previous models for the spin-down behavior of intermittent pulsars (Beskin & Nokhrina 2007; Li et al. 2012) may also be applied to the variable spin-down rate of PSR B0540−69. However, the expected braking index is three in Beskin & Nokhrina (2007) and related magnetohydrodynamical simulations (Li et al. 2012). Considering the effects of pulsar death or evolution of inclination angle, the braking index will be larger than three (Contopoulos & Spitkovsky 2006; Philippov et al. 2014). Therefore, these models should be modified before they can explain both the persistent state braking index and variable spin-down rate of PSR B0540−69.

There are several models designed for magnetar spin-down which may also be employed in the case of PSR B0540−69. The magnetar spin-down may be dominated by a particle wind (Harding et al. 1999). The calculations in Harding et al. (1999) assume each particle in the outflow can attain the maximum acceleration potential of a rotating dipole (Tong et al. 2013). This wind braking model of magnetars was employed by Kramer et al. (2006) to explain the spin-down behavior of the first intermittent pulsar PSR B1931+24. An additional particle outflow in the on state will result in a larger spin-down rate. The rotational energy loss is related to the particle wind luminosity $L_{\rm p}$ as $\propto \sqrt{L_{\rm p}}$ (Harding et al. 1999). A particle wind luminosity that is 85% will result in a spin-down rate that is 36%. The particle wind luminosity is related to the polar cap radius $R_{\rm pc}$ and magnetospheric opening radius $r_{\rm open}$ as $L_{\rm p} \propto R_{\rm pc}^4 \propto r_{\rm open}^{-2}$ (Harding et al. 1999). Therefore, the magnetospheric opening radius will be 26% smaller. However, there are several problems when applying the wind braking model of magnetars to the case of normal pulsars:

(1) In the wind braking model of magnetars, a strong particle wind is assumed. The effect of magnetic dipole radiation is neglected. This may be applicable to the case of magnetars whose emissions are dominated by magnetic energy output (Tong et al. 2013). However, in the case of normal pulsars (including intermittent pulsars), the effect of dipole radiation may not be neglected.
(2) In the case of strong particle wind, the braking index is $n = 1$ (Tong et al. 2013). This is not consistent with the braking index of pulsars (Lyne et al. 2015).
(3) When applying to the case of intermittent pulsars (Kramer et al. 2006; Young et al. 2013), pure magnetic dipole braking is assumed for the off state. This may be valid for the case of intermittent pulsars whose radio emissions are stopped in the off state (Li et al. 2014). However, this assumption cannot be applied to the persistent spin-down state of PSR B0540−69 which still has multiwavelength emissions.

The twisted magnetosphere model of magnetars (Thompson et al. 2002) has showed that the effective magnetic field will be larger for a larger twist. If the magnetosphere of PSR B0540−69 is twisted by a glitch, then it will also result in a larger spin-down rate. However, the twisted magnetosphere will relax back to the pure magnetic dipole case in several years (Beloborodov 2009). During this process, the neutron star's X-ray luminosity and spin-down rate will both decrease with time. For PSR B0540−69, its high spin-down state has lasted more than 3 years (Marshall et al. 2015). This is inconsistent with the expectation of the twisted magnetosphere model.

There are also external models for the braking index or intermittent pulsar spin-down behavior, e.g., the fall-back disk model (Liu et al. 2014 and references therein; Li 2006). However, these external models are hard to verify or falsify. Furthermore, accretion will halt the magnetospheric activities. In the presence of accretion, it may be difficult to reconcile the measured braking index with radio emissions from PSR B0540−69 and other pulsars.

Observations of the timing behavior and pulse profile of some pulsars indicate that the $\dot{\nu}$ modulation and the pulse-shape variation are correlated, e.g. PSR B0910+16 (Perera et al. 2015) and PSR B1859+07 (Perera et al. 2016). This relation indicates that both these phenomena are magnetospheric in origin (Lyne et al. 2010). A theory of a variable particle density in the magnetosphere has been successfully applied to explain the spin-down behavior and emission properties of an intermittent pulsar (Kramer et al. 2006; Li et al. 2014). The mode changing and nulling in a pulsar may be understood similarly because of the detection of variation in spin-down rate of PSR J1717−4054 (Young et al. 2015) and a weak emission state in addition to the bright and nulling states of PSRs J1853+0505 and J1107-5907 (Young et al. 2014). For PSR B0540−69, the increase of particle density in the magnetosphere will change the spin-down rate, as well as the pulse profile. The giant radio pulse of PSR B 0540−69 (Johnston et al. 2004) could have been caused by a larger outflowing particle density. In addition, different emission models (core, cone and patch) are applied to explain the variable mean pulse profiles (Lyne & Manchester 1988). It is predicted that the corotation of the magnetosphere with a pulsar may also affect its emission properties (Wang et al. 2012b). Hence, the nonuniform distribution of particles between these core and conal components will also change the pulse shape. For PSR B0540−69, the pulse profile has a broad double peak which can be described by two Gaussians with a phase separation of 20% (de Plaa et al. 2003). We should emphasize that: (i) if the particles are distributed uniformly, the increase in outflowing particle density may result in an increase of pulse intensity such that the ratio of these two components stays constant; (ii) if the particles are distributed nonuniformly, both the pulse intensity and the ratio will change; (iii) the coherent manner in which particles are radiated may affect the pulse shape as well. The pulse profile and total flux in the high spin-down state are needed in order to compare them with the low spin-down state.

4 CONCLUSIONS

The pulsar wind model is applied to explain the variable timing behavior of PSR B0540−69 and PSR J1846−0258. Both the persistent state braking index and the variable spin-down rate of PSR B0540−69 are understandable with this model. A larger particle density will result in an increase in the spin down rate and predicts a smaller braking index. An increasing particle density will lead to a lower braking index. For PSR B0540−69, in the vacuum gap model, corresponding to the 36% increase in the spin-down rate, the relative increase in particle density is 88%. The braking index decreases to 1.79. The same conclusion is obtained for different acceleration models. Since measurements have revealed both a variable spin-down rate and persistent state braking index, PSR B0540−69 is very powerful in constraining different pulsar spin-down mechanisms. Future observations of the braking index in the new spin-down state will provide further tests on different spin-down models and different particle acceleration models in the wind braking scenario. For PSR J1846−0258, the variable timing behavior showing a net decrease in spin down frequency ($\Delta\nu \approx -10^{-4}\,\mathrm{Hz}$) can be understood similarly. A changing rate of particle density $\dot{\kappa} = 1.68 \times 10^{-9}\,\mathrm{s}^{-1}$ will result in a lower braking index of 2.19.

Acknowledgements The authors would like to thank R.X. Xu for discussions. H. Tong is supported by the West Light Foundation of CAS (LHXZ 201201), the 973 Program (2015CB857100) and Qing Cu Hui of CAS.

References

Archibald, R. F., Kaspi, V. M., Beardmore, A. P., Gehrels, N., & Kennea, J. A. 2015a, ApJ, 810, 67
Archibald, R. F., Kaspi, V. M., Ng, C.-Y., et al. 2015b, ApJ, 800, 33
Becker, W. 2009, in Astrophysics and Space Science Library, 357, Astrophysics and Space Science Library, ed. W. Becker, 91
Beloborodov, A. M. 2009, ApJ, 703, 1044
Beskin, V. S., & Nokhrina, E. E. 2007, Ap&SS, 308, 569
Contopoulos, I., & Spitkovsky, A. 2006, ApJ, 643, 1139
Cusumano, G., Massaro, E., & Mineo, T. 2003, A&A, 402, 647
de Plaa, J., Kuiper, L., & Hermsen, W. 2003, A&A, 400, 1013
Espinoza, C. M., Lyne, A. G., Kramer, M., Manchester, R. N., & Kaspi, V. M. 2011, ApJ, 741, L13
Ferdman, R. D., Archibald, R. F., & Kaspi, V. M. 2015, ApJ, 812, 95
Gavriil, F. P., Gonzalez, M. E., Gotthelf, E. V., et al. 2008, Science, 319, 1802
Goldreich, P., & Julian, W. H. 1969, ApJ, 157, 869
Harding, A. K., Contopoulos, I., & Kazanas, D. 1999, ApJ, 525, L125
Johnston, S., Romani, R. W., Marshall, F. E., & Zhang, W. 2004, MNRAS, 355, 31
Kou, F. F., & Tong, H. 2015, MNRAS, 450, 1990
Kramer, M., Lyne, A. G., O'Brien, J. T., Jordan, C. A., & Lorimer, D. R. 2006, Science, 312, 549
Li, J., Spitkovsky, A., & Tchekhovskoy, A. 2012, ApJ, 746, L24
Li, L., Tong, H., Yan, W. M., et al. 2014, ApJ, 788, 16
Li, X.-D. 2006, ApJ, 646, L139
Liu, X.-W., Xu, R.-X., Qiao, G.-J., Han, J.-L., & Tong, H. 2014, RAA (Research in Astronomy and Astrophysics), 14, 85
Livingstone, M. A., Kaspi, V. M., & Gavriil, F. P. 2005, ApJ, 633, 1095
Livingstone, M. A., Kaspi, V. M., & Gavriil, F. P. 2010, ApJ, 710, 1710
Livingstone, M. A., Kaspi, V. M., Gotthelf, E. V., & Kuiper, L. 2006, ApJ, 647, 1286
Livingstone, M. A., Ng, C.-Y., Kaspi, V. M., Gavriil, F. P., & Gotthelf, E. V. 2011, ApJ, 730, 66
Lyne, A. G., Jordan, C. A., Graham-Smith, F., et al. 2015, MNRAS, 446, 857
Lyne, A. G., & Manchester, R. N. 1988, MNRAS, 234, 477
Lyne, A., Graham-Smith, F., Weltevrede, P., et al. 2013, Science, 342, 598
Lyne, A., Hobbs, G., Kramer, M., Stairs, I., & Stappers, B. 2010, Science, 329, 408
Marshall, F. E., Guillemot, L., Harding, A. K., Martin, P., & Smith, D. A. 2015, ApJ, 807, L27
Perera, B. B. P., Stappers, B. W., Weltevrede, P., Lyne, A. G., & Bassa, C. G. 2015, MNRAS, 446, 1380
Perera, B. B. P., Stappers, B. W., Weltevrede, P., Lyne, A. G., & Rankin, J. M. 2016, MNRAS, 455, 1071
Philippov, A., Tchekhovskoy, A., & Li, J. G. 2014, MNRAS, 441, 1879
Ruderman, M. A., & Sutherland, P. G. 1975, ApJ, 196, 51
Thompson, C., Lyutikov, M., & Kulkarni, S. R. 2002, ApJ, 574, 332
Tong, H. 2015, arXiv:1506.04605
Tong, H., Xu, R. X., Song, L. M., & Qiao, G. J. 2013, ApJ, 768, 144
Wang, J., Wang, N., Tong, H., & Yuan, J. 2012a, Ap&SS, 340, 307
Wang, P. F., Wang, C., & Han, J. L. 2012b, MNRAS, 423, 2464
Wu, F., Xu, R. X., & Gil, J. 2003, A&A, 409, 641
Xu, R. X., & Qiao, G. J. 2001, ApJ, 561, L85
Young, N. J., Stappers, B. W., Lyne, A. G., et al. 2013, MNRAS, 429, 2569
Young, N. J., Weltevrede, P., Stappers, B. W., Lyne, A. G., & Kramer, M. 2014, MNRAS, 442, 2519
Young, N. J., Weltevrede, P., Stappers, B. W., Lyne, A. G., & Kramer, M. 2015, MNRAS, 449, 1495
Yue, Y. L., Xu, R. X., & Zhu, W. W. 2007, Advances in Space Research, 40, 1491
Zhang, L., & Cheng, K. S. 2000, A&A, 363, 575
Zhang, W., Marshall, F. E., Gotthelf, E. V., Middleditch, J., & Wang, Q. D. 2001, ApJ, 554, L177
Zhou, E. P., Lu, J. G., Tong, H., & Xu, R. X. 2014, MNRAS, 443, 2705